

Emulsion electrospun PLA/calcium alginate nanofibers for periodontal tissue engineering

Journal of Biomaterials Applications
2020, Vol. 34(6) 763–777
© The Author(s) 2019
Article reuse guidelines:
sagepub.com/journals-permissions
DOI: 10.1177/0885328219873561
journals.sagepub.com/home/jba



Zhanchao Ye^{1,*}, Weihong Xu^{1,2,*}, Renze Shen¹  and Yurong Yan²

Abstract

Objective: The regeneration of periodontal bone tissue is a major obstacle in tissue engineering. We have recently designed a compound nanofiber scaffold for the tissue repair of periodontal bone, which was composed of poly(lactic acid) (PLA) and calcium alginate (CA). The obtained improvements in both physical properties and biological effects on periodontal tissue were systematically evaluated and discussed.

Method: Neat PLA and PLA/CA nanofiber scaffolds were prepared by electrospinning technology. Scanning electron microscopy was applied for the observation of surface morphology. Their mechanical properties were evaluated in terms of elongation at break and elastic modulus. Hydrophilic/hydrophobic nature of the nanofibers was investigated by a stereomicroscope, and their *in vitro* degradation was tested as well. Cell proliferation and adhesion were detected in order to evaluate the biocompatibility of nanofiber scaffolds. Expression of cell mineralization gene and formation of mineralization knots were examined so as to assess scaffolds' capability of regenerating bone tissues. The expression of Toll-like receptor 4 (TLR4), IL-6, IL-8, and IL-1 β was utilized to decide the possibility of tissue inflammation caused by the nanofibers with the assistance of reverse transcription-polymerase chain reaction (RT-PCR) assay.

Results: The obtained nanofibers possessed uniform surface morphology. The elongation at break and elastic modulus of PLA/CA nanofiber scaffolds were higher than those of neat PLA. CA could enhance the hydrophilicity of PLA fibers; in the meantime, it promoted cell adhesion of periodontal ligament cells (PDLCs) and bone marrow stromal cells (BMSCs). Addition of CA had raised the expression level of cell mineralization gene and the formation of mineralization knots (BMSCs). On the other hand, both neat PLA fibers and PLA/CA fibers could induce higher expression level of inflammatory mediators and TLR4 of human periodontal ligament cells (hPDLCs).

Conclusions: The introduction of CA enhanced the mechanical properties of neat PLA nanofibers and increased its hydrophilicity. Neat PLA nanofibers and PLA/CA scaffold could both facilitate BMSCs proliferation, while the addition of CA promoted BMSCs osteogenic differentiation. The improved (or enhanced) expression of inflammatory mediators caused by nanofibers might be regulated via TLR4 pathway.

Keywords

Poly(lactic acid), toll-like receptor 4, calcium alginate, periodontal bone tissue

Introduction

Chronic periodontitis is a multi-factorial infectious disease characterized by slow but irreversible damage of periodontal supporting tissue loss over time.¹ The loss

*These authors contributed equally to this study and should be considered as co-first authors.

Corresponding authors:

Renze Shen, Department of Stomatology, Zhongshan Hospital of Xiamen University, Medical College of Xiamen University, Xiamen University, Xiamen 361000, China.
Email: KQSRZ123@163.com

Yurong Yan, Department of Polymer Materials and Engineering, South China University of Technology, Guangzhou 510640, People's Republic of China.
Email: yryan@scut.edu.cn

¹Department of Stomatology, Medical College of Xiamen University, Zhongshan Hospital of Xiamen University, Xiamen University, Xiamen, China

²Department of Polymer Materials and Engineering, South China University of Technology, Guangzhou, China

of periodontal supporting tissues in a period of time can lead to more difficulties in denture repair and a higher failure rate of implant repair. For patients with advanced periodontal breakdown, periodontal surgery has become increasingly essential to obtain significant gain in attached gingiva and keratinized gingiva.² Nevertheless, the regeneration of periodontal bone tissue via such kind of surgery remains difficult. Guided bone regeneration (GBR) has shown favorable advantages in periodontal bone regeneration, and even furcation area defects,^{3,4} and the advancements in related biomaterials have further improved its therapeutic effect,⁵ such as tricalcium phosphate, hydroxyapatite, fresh-frozen bone allografts, etc. To date, there is not yet any ideal option for the biomaterial that can continuously provide perfect clinical results with regard to periodontal regeneration. Further extensive research is required with focus on the improvement of biological interface between graft materials and host tissues.⁵ A good material structure is one of the most essential factors, for it is conducive to cell proliferation, differentiation induced by bone tissues, and sufficient mechanical strength that meets the space requirement for tissue growth.

Scaffolds made from the same material but with different structures may exhibit varied effects on bone tissue growth, which is primarily because scaffold structure can affect the adhesion and growth direction of cells. It has been reported that the organized scaffold architecture could provide topographic cues to the adherent cells, thus they would proliferate along its axes.^{6,7} The ability to guide cellular alignment on scaffolds in a specialized direction is advantageous for tissue regeneration, such as the periodontal ligament.⁷ Via implanting cells on nanofibers and applying mechanical stress, it was found that the cells could recognize the nanofiber orientation and align in parallel, and the mechanical stress benefited cell alignment.⁸ Other experiments confirmed that composite nanofibers were helpful to promote bone regeneration in furcation defects, and could provide a basis for the potential application as GTR/GBR membranes.⁹ Therefore, nanofibers were chosen as the scaffold structure in this study.

PLA, a biocompatible material, has been used in tissue engineering for years as a very popular option.^{10–12} However, its hydrophobicity along with the acidic degradation products hinders its more extensive usage. CA exhibits good ability to induce bone regeneration as well as low cytotoxicity, high hydrophilicity, and high alkalinity,^{13–16} while it is mechanically brittle and hardly exists with fibrous structure. By combining PLA with CA, the pH value of the composite material, its hydrophilicity, and its mechanical strength

might be tuned. A scaffold suitable for tissue growth can thus be prepared.

In this study, neat PLA and PLA/CA nanofibers were fabricated. The surface structure of the materials was observed by scanning electron microscopy, and the hydrophilicity, mechanical properties, vitro degradation nature of the nanofibers were subsequently measured. Cell adhesion and proliferation were tested to determine their biocompatibility, while osteogenic differentiation of BMSCs was examined to evaluate the pro-regenerative capacity of the scaffolds. Finally, the mRNA level of TLR4, IL-6, IL-8, IL-1 β of periodontal ligament cells was detected in order to study the pro-inflammatory ability of the nanofibers.

Experimental

Materials

Preparation of PLA/CA nanofiber scaffolds. Firstly, SA (sodium alginate) was dissolved in distilled water with a concentration of 40 mg/mL, and Span80 (0.3 g) was added in 10 mL of chloroform. Secondly, the obtained SA solution with various amounts was added respectively into the Span80/chloroform solution under a high stirring speed of 7000 r/min for 10 min. PLA was then added into the mixed solution and the mixture was further stirred at 240 r/min for 2 h to obtain uniform emulsions. Emulsions were placed in a horizontally positioned plastic syringe (1 mL) with a flat-end metal needle (0.6 mm in inner diameter), respectively. Then, the syringe was operated with the assistance of a syringe pump to feed solution at a rate of 0.5 ml/h. Besides, the needle was subjected to a high-voltage DC power of 15 kV. The collector was placed 15 cm clear of the needle tip, which was covered by a sheet of aluminum foil for the collection of fibers. Electrospinning of nanofibers with varied PLA/SA ratios was subsequently carried out referring to the literature.¹⁷ Lastly, the obtained PLA/SA membranes were transformed into PLA/CA ones via three methods based on the ion exchange of Na⁺ with Ca²⁺: (1) 1 mL of CaCl₂ solution (0.2 g/mL) was sprayed to the PLA/SA membrane (Sample 1); (2) 2 mL of CaCl₂ solution (0.2 g/mL) was sprayed to the PLA/SA membrane (Sample 2); (3) the PLA/SA membrane was immersed into 100 mL of CaCl₂ solution (0.01 g/mL) (Sample 3).

Physical tests

Mechanical property test. The neat PLA and PLA/CA nanofiber scaffolds were cut into strips with 30 mm \times 1 mm in dimension and tested by an YGOO4D Single Fiber Strength Tester (Changzhou Second Textile Machines Co., Ltd, China) at ambient

condition. At least 15 measurements were carried out for each sample, and the average value was recorded as the final result.

Hydrophilicity test. Water contact angle was examined to evaluate the hydrophilic/hydrophobic nature of the scaffold. Samples were dried overnight at 60°C in a vacuum oven before 8 µL of water/ink was dropped onto them. A stereomicroscope was placed in front of the sample holder to capture the droplet geometry, and the average value of 15 samples was recorded as the final result.

Vitro degradation and pH value tests. Two methods were utilized to measure the scaffold degradation. For the first, 50 mg of each sample ($n = 15$) was cut into small pieces and immersed in 50 mL of phosphate-buffered saline (PBS, pH = 7.4) at 37°C and a shaking speed of 120 r/min. During testing, the scaffolds were dried and weighed while PBS was refreshed, and the pH change of PBS was traced throughout the whole degradation process. The second method is the same as that mentioned above except for no shaking.

Water absorption test. Water absorption of the scaffolds was measured according to the British Pharmacopoeia Monograph. To achieve a constant weight, all the samples were dried in a vacuum oven overnight at room temperature. Then they were cut into appropriately-sized strips and weighed to record the initial weights (W_0). For measurement, all samples were immersed into distilled water of 37°C for up to 12 and 24 h. The wet samples were picked out and hung up with a pair of forceps for 30 s before weighed (W_1). Then they were weighed again after drying at 60°C for 24 h to become completely dried samples (W_3). The water holding capacity (WHC) and water absorption capacity (WAC) were calculated as

$$\text{WHC} = (W_0 - W_3) / W_3$$

$$\text{WAC} = (W_1 - W_3) / W_3$$

Biological tests

Morphologies of BMSCs. The electrospun fibers (neat PLA, Samples 1, 2, and 3) were cut into small wafers with diameter of 15.6 mm. After sterilized with 75% alcohol and ultraviolet (UV) light, the samples were washed three times with PBS for 20 min to eliminate cytotoxicity caused by any residual solvent. Then the fiber samples were mounted at one piece per well in a 24-well plate, while the cells were detached, counted, and seeded on these samples. After co-culturing for

24 h, each piece of fibers with cells was fixed, washed with PBS, and dehydrated. At last, all the samples were air-dried and stored for further SEM test.

BMSCs proliferation and differentiation assay

BMSCs proliferation assay. The fibers and cells were treated with the above-mentioned methods. MTT (4,5-dimethyl-2-thiazolyl)-2,5-diphenyl-2-*H*-tetrazolium bromide) test was applied to evaluate cell proliferation. Cells were incubated for one, three, five, and seven-days, respectively, followed by incubation for another 4 h at 37°C after adding 50 µL of MTT aqueous solution (mg/mL). Then DMSO was added into each culture plate, which was shaken for 10 min with protection from light. Mixed solutions (150 µL) from each well of the 24-well plate were transferred separately to 96-well plates, and a microplate spectrophotometer (model 680; Bio-Rad Laboratories, Hercules, CA) was used to examine each well at an absorbance of 490 nm. The cells inoculated on a culture plate regarded as NC (natural control group).

BMSCs differentiation assay. The fibers and cells were treated with the above-mentioned methods. Cells were cultured for 14 days in an osteogenic medium and then stained by Alizarin Red to determine the cell mineralization degree. The scaffolds with cells attached were washed with PBS for three times, fixed in 4% (v/v) paraformaldehyde for 10 min, and stained with 5% Alizarin Red for 15 min. Cells were rinsed off for observation with a microscope (Nikon TS-100, Japan). The mRNA level of mineralization genes was tested by real-time polymerase chain reaction (RT-PCR) and the total cellular mRNA was obtained from cells using trizol (Takara, Kyoto, Japan) according to manufacturer's recommendations. Reverse transcription was performed by the PrimeScriptR reagent kit (Takara, Kyoto, Japan), while the cDNA levels were measured by RT-PCR using the SYBRR Premix DimerEraser™ kit (Takara, Kyoto, Japan). All genes were analyzed using the Applied Biosystems 7500 Real-Time PCR System (Applied Biosystems, USA).

hPDLcs proliferation and inflammation assay

Preparation and identification of hPDLcs. Primary hPDLcs were cultured, identified, and utilized in this study referring to the methods previously reported by our group.^{16,18}

Cytoactivity test of hPDLcs. Same operations as those in BMSCs proliferation assay were carried out except that hPDLcs were involved here instead of BMSCs.

hPDLcs inflammation assay. The fibers and cells were treated with the above-mentioned methods. Detached cells were centrifuged, counted, and seeded on the scaffolds for seven days. Tissue culture plate (TCP) was utilized as a control group. The mRNA level of inflammation genes was tested by RT-PCR, and the inflammation genes including IL-6, IL-8, and TLR4 were test.

Results

Morphology of fibers

Figure 1 shows that PLA, PLA/SA, and PLA/CA fibers were all continuous with uniform diameters. After soaked in water, the surface structure of PLA/SA fibers was damaged due to SA dissolution (Figure 1 (d)), whereas that of PLA/CA fibers remained intact since CA could not dissolve in water (Figure 1(e)).

Figure 2 presents the SEM micrographs of neat PLA and PLA/CA fibers made by three methods. It can be seen that the fibers exhibited uniform diameters without any beaded structure. The fiber diameters of neat

PLA fibers were (780 ± 200) nm, and those of PLA/CA1, PLA/CA2, PLA/CA3 were about (250 ± 90) nm.

Physical properties of neat PLA and PLA/CA fibers

Mechanical performance of neat PLA and PLA/CA fibers. The elastic modulus of PLA fibers was about (0.27 ± 0.02) MPa. Ion exchange reaction raised this value of PLA/CA fibers for about five times, reaching up to PLA/CA1 (1.34 ± 0.08) MPa, PLA/CA2 (1.32 ± 0.31) MPa, PLA/CA3 (1.78 ± 0.11) .

Tensile stress of the initial PLA fibers was (0.25 ± 0.03) MPa, while that of the PLA/CA fibers increased more than five times. PLA/CA1 (1.36 ± 0.10) MPa, PLA/CA2 (1.41 ± 0.34) MPa, PLA/CA3 (3.13 ± 0.24) .

PLA fibers possessed an elongation at break about $(31.2 \pm 4.7)\%$, and PLA/CA fibers showed a higher value. PLA/CA1 $(79.3 \pm 7.6)\%$, PLA/CA2 (85 ± 0.53) MPa, PLA/CA3 $(110.8 \pm 10.9)\%$. Thus, the elastic modulus, tensile stress, and elongation at break of

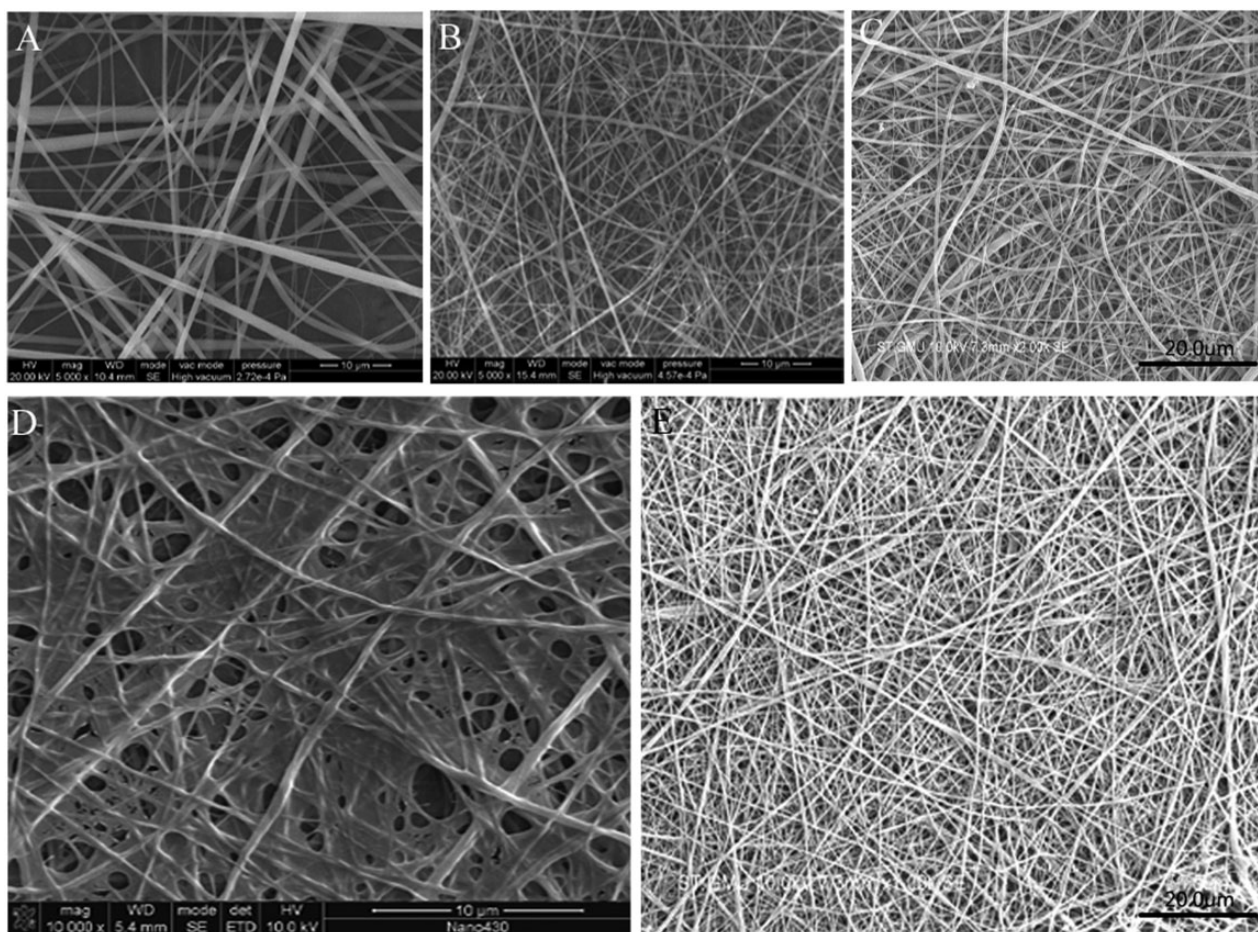


Figure 1. The morphology of neat PLA, PLA/SA, and PLA/CA fibers (SEM) (a) PLA; (b) PLA/SA (9:1); (c) PLA/CA and (d) PLA/SA soaked in water; (e) PLA/CA soaked in water.

PLA/CA were all enhanced when compared with the original neat fibers.

Water absorption of neat PLA and PLA/CA fibers. Figure 3 demonstrates WAC and WHC of the scaffolds. It was proved that both of them were improved by adding CA. The WAC and WHC of PLA/CA1, PLA/CA2 and PLA/CA3 were found to be significantly higher than those of pure PLA group. Nevertheless, there was no noticeable difference observed between PLA/CA1, PLA/CA2 and PLA/CA3. It is demonstrated that PLA/CA fibers derived from applying the three methods are effective in making substantial improvement to the WAC and WHC of pure PLA fibers.

Water contact angle of neat PLA and PLA/CA fibers. Figure 4 gives the results for water contact angle measurement, which reveals a significant reduction trend in water contact angles by adding CA. This suggests the increase in fibers' wettability.

Degradation rate of neat PLA and PLA/CA fibers. Figure 5(a) to (h) describes the morphology of neat PLA and PLA/CA fibers during degradation. It can be observed from Figures 5(b) and 6(a) that the scaffolds were

more likely to fracture into pieces when shaking was applied.

Change of pH values during degradation of neat PLA and PLA/CA fibers. As shown in Figure 7, adding CA did not increase the pH values of PLA fibers during degradation in PBS. All scaffolds, including the neat one, had hardly decreased pH values of PBS.

Biological tests of neat PLA and PLA/CA fibers

Histochemical staining of cells grown on fibers. Figure 8 shows the morphology of the actual native tissue of periodontal tissues, such as alveolar bone and cementum. Figure (8a) shows the HE staining of periodontal membrane, which can show the structure of cells and surrounding microenvironment in periodontal membrane. Collagen fibers are represented by red staining in Figure (8b) and blue staining in Figure (8c). You can see that the periodontal membrane is basically composed of fibers of collagen. The staining of alveolar bone with teeth is shown in Figure 8(d) and (e). It can be seen that both bone tissue and periodontal membrane growth microenvironment contain a lot of fibers. Cells grow in microenvironments made up of fibers.

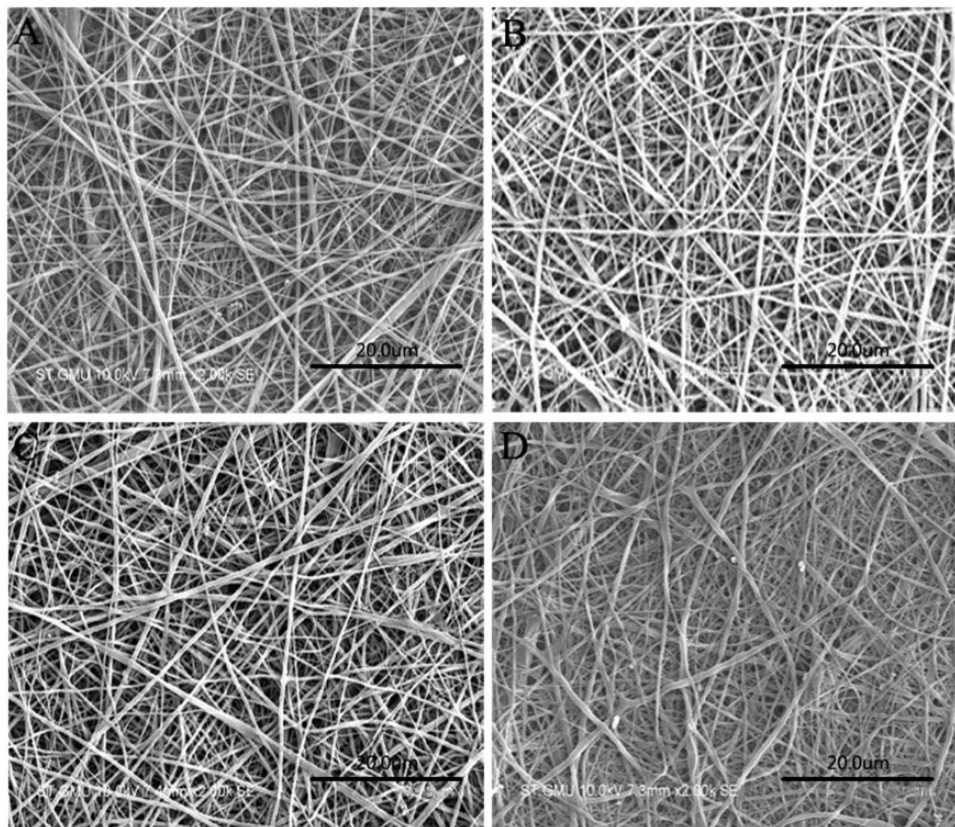


Figure 2. The morphology of neat PLA and PLA/CA fibers (SEM) (a) PLA; (b) PLA/CA1; (c) PLA/CA2 and (d) PLA/CA3.

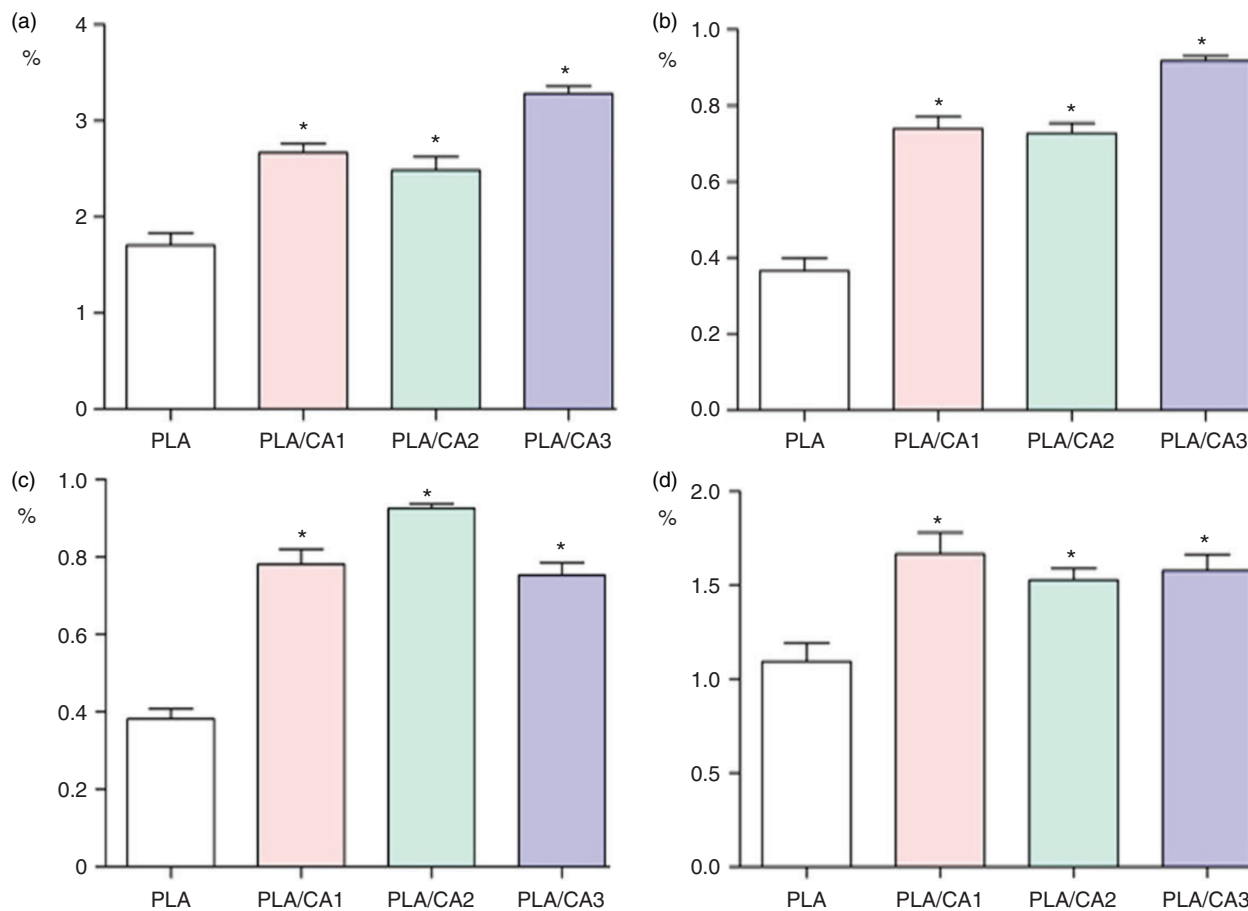


Figure 3. Water absorption testing of fibers: (a) WAC of 12 h; (b) WAC of 24 h; (c) WHC of 12 h and (d) WHC of 24 h ($*P < 0.05$, *represents a statistically significant difference with the NC group).

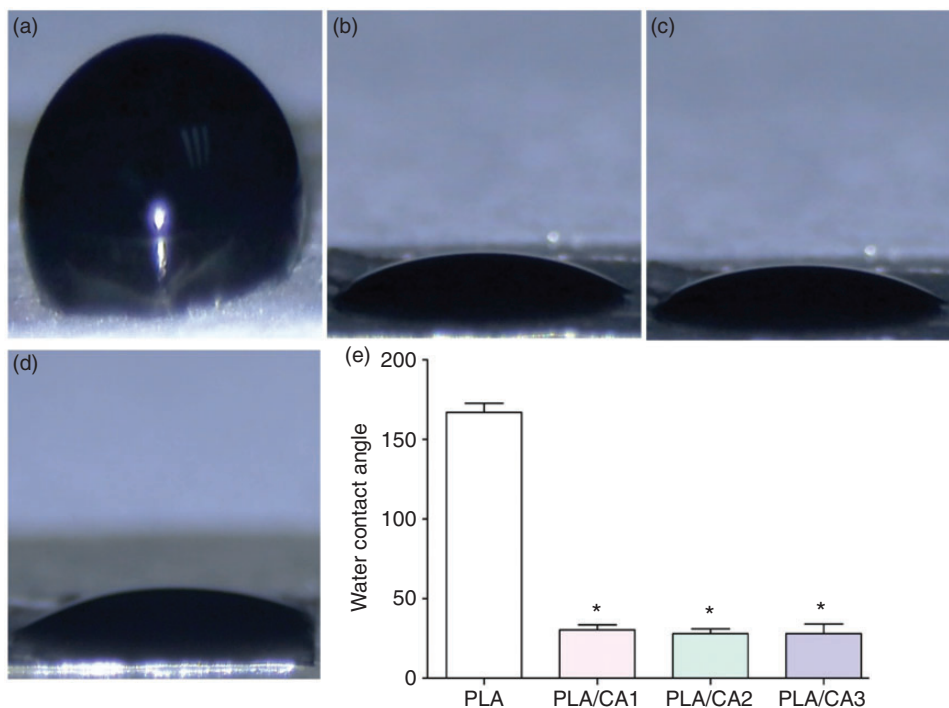


Figure 4. Water contact angle of neat PLA and PLA/CA fibers stereomicroscope ($\times 6$) (a) PLA; (b) PLA/CA1; (c) PLA/CA2; (d) PLA/CA3 and (e) Summary of water contact angles ($*P < 0.05$, *represents a statistically significant difference with the NC group).

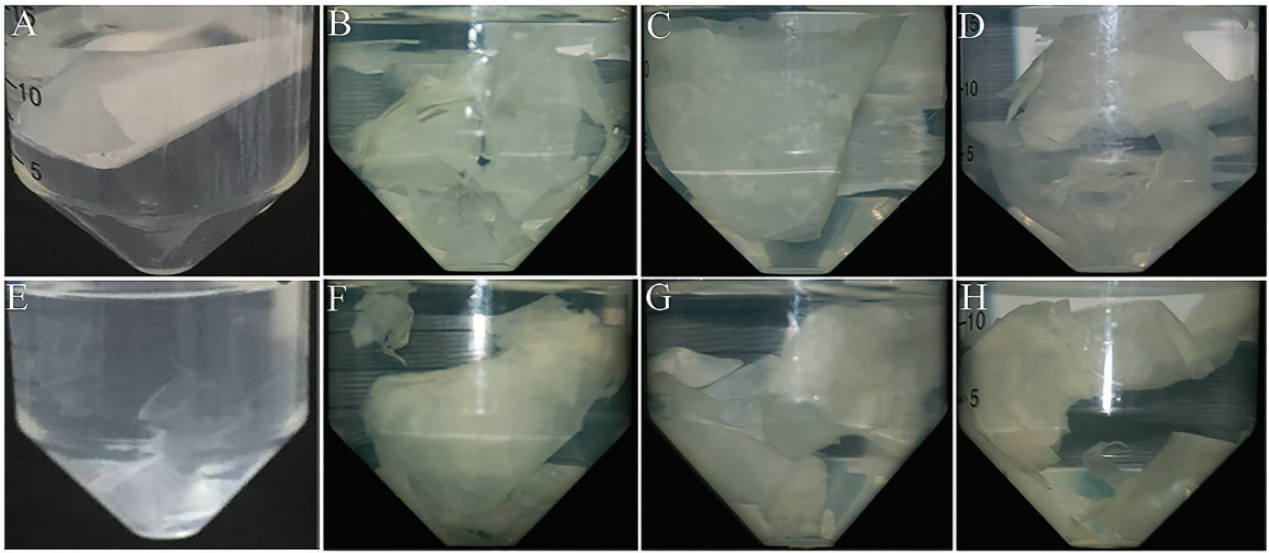


Figure 5. Degradation of electrospun fibers: morphology of fibers (stereomicroscope $\times 6$); (a) PLA, (b) PLA/CA1, (c) PLA/CA2, and (d) PLA/CA3 fibers immersed in PBS for 24 h without shaking; morphology of (e) PLA, (f) PLA/CA1, (g) PLA/CA2, and (h) PLA/CA3 fibers immersed in PBS for 24 h with shaking.

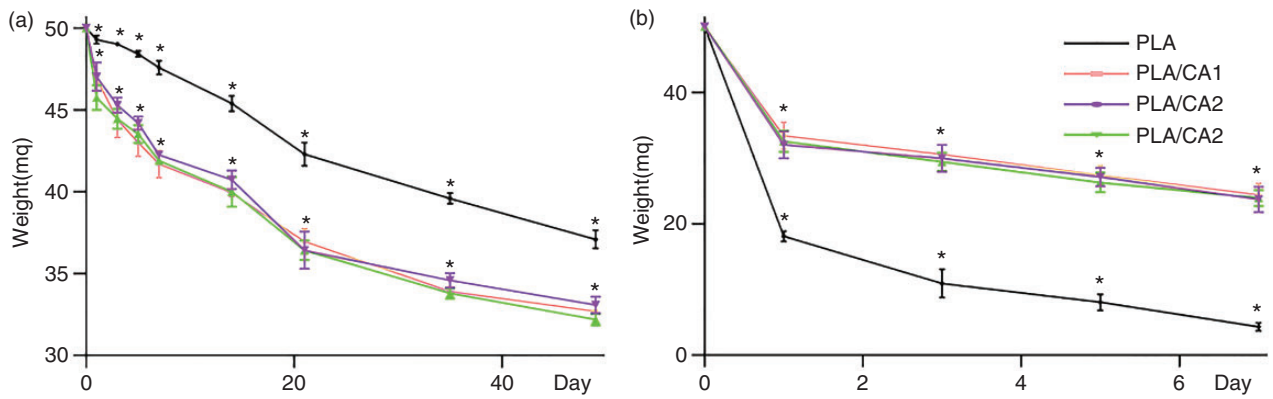


Figure 6. Degradation of electrospun fibers: (a) Degradation of electrospun fibers without shaking and (b) Degradation of electrospun fibers with shaking.

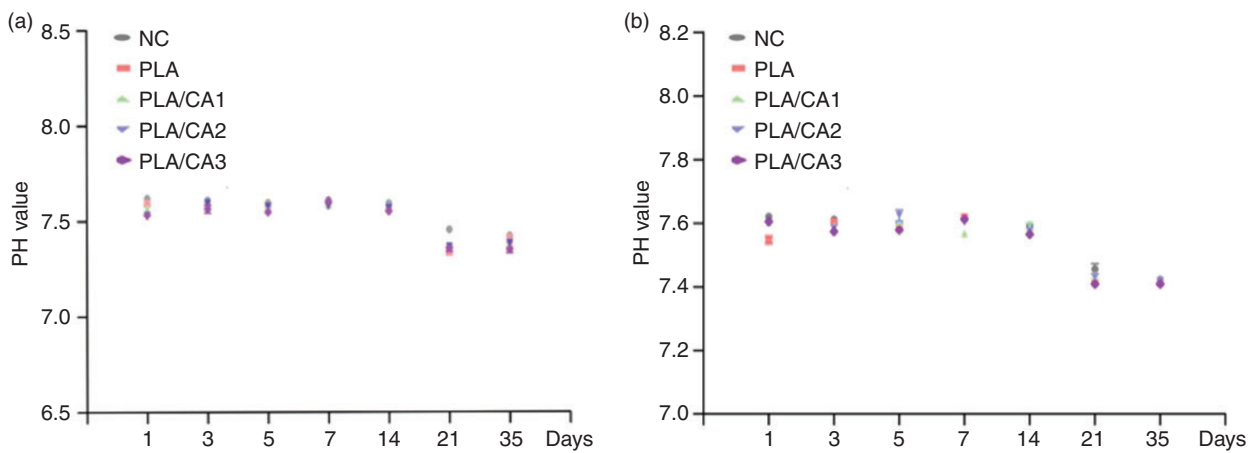


Figure 7. pH variation of fibers (a) without and (b) with shaking.

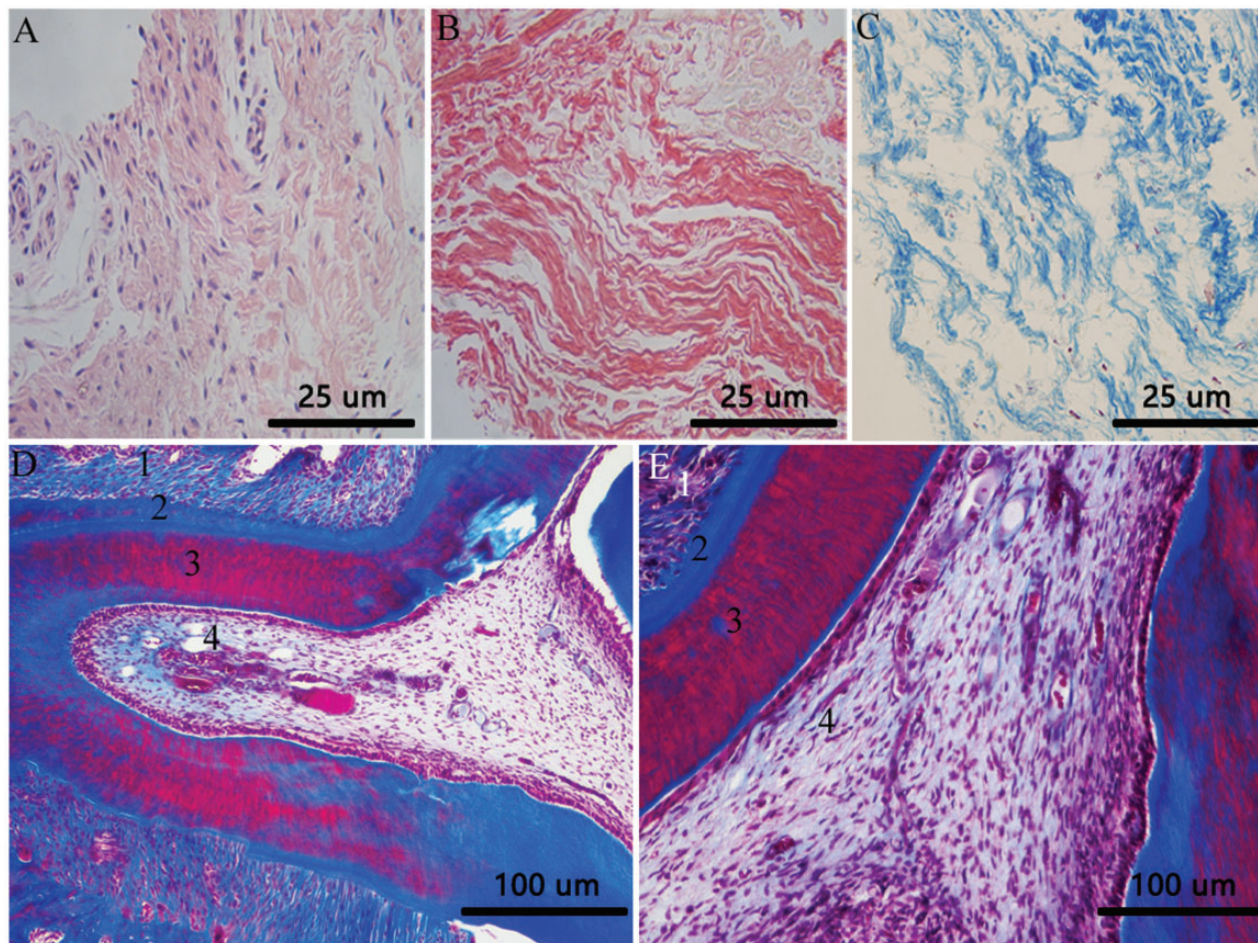


Figure 8. Histochemical staining of periodontal tissue (optical microscope): (a) HE, (b) Sirius Red, and (c) Masson staining of human periodontal tissue (25 \times); Masson staining of rat periodontal tissue at (d) 25 \times and (e) 100 \times (1 alveolar bone; 2 periodontal ligament; 3 dentin and cementum; 4 dental pulp).

Scanning electron microscopy of cell growth in periodontal tissue. In Figure 8, it can be observed that hPDLCs and BMSCs grow in a fibrous environment filled with collagen fibers. The scaffold structure shown in Figure 9 is also fibrous, exhibiting similarity to the collagen fibers derived from the cell.

SEM images revealed the morphologies of BMSCs attached to scaffolds (Figure 9). The surface of scaffolds was covered by cells, while their uniform structure was retained. Cells spread with pseudopodia, indicating good adhesion and activity.

BMSCs proliferation assay. During the first three days, OD value of the fiber group was significantly higher than that of the blank control group (Figure 10), and PLA/CA fibers possessed higher values than neat PLA fibers did. However, the cell proliferation in the experimental group was not clearly superior to that in the NC group at days 5–7, when the cells in the experimental

group have a possibility to have experienced premature growth. Due to insufficient space, growth was inhibited in the experimental group.

Assessment of BMSCs osteoinductive capacity by alizarin red staining. As demonstrated in Figure 11, cells cultured on PLA/CA nanofibers exhibited clear matrix mineralization with more intense ARS compared with the PLA group.

Assessment of BMSCs osteoinductive capacity by mineralized gene expression detection. Figure 12 illustrates the quantification of mineralization-related genes by real-time PCR, which suggested that PLA/CA nanofibers could enhance the expression levels of mineralization genes including Runx2, OPG, Collagen I, and RANKL.

hPDLCs proliferation assay. Similar to BMSCs proliferation, OD value of the fiber group was significantly

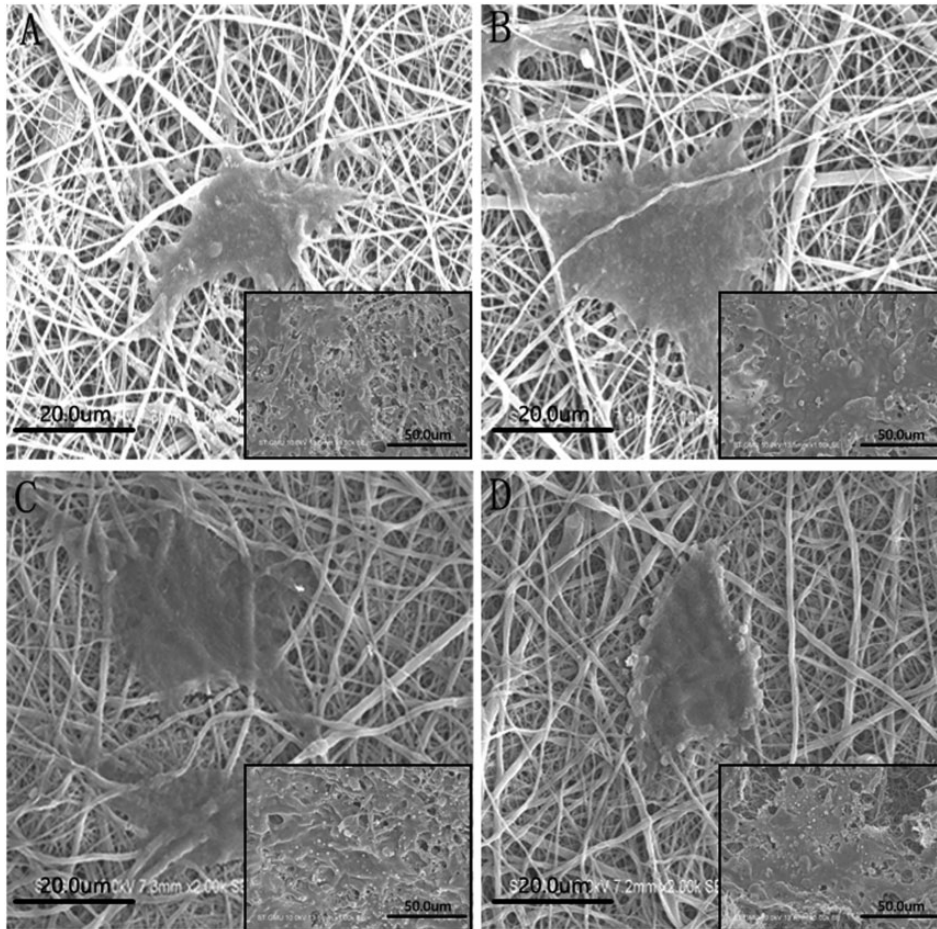


Figure 9. Morphology of BMSCs seeded on fibers (SEM): (a) PLA; (b) PLA/CA1; (c) PLA/CA2 and (d) PLA/CA3.

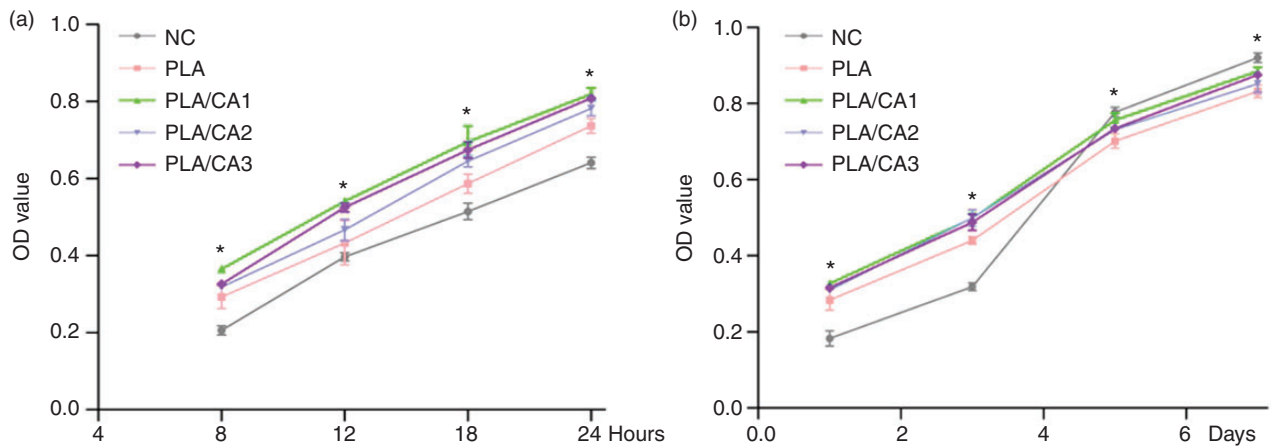


Figure 10. Proliferation of BMSCs seeded on fibers (* $P < 0.05$, *represents a statistically significant difference with the NC group).

higher than that of the TCP group during the first three days, with PLA/CA fibers' higher than neat PLA fibers'. However, the OD value of fiber group was not higher any more in the later stage (Figure 13).

hPDLs inflammation assay. Cells being seeded on scaffolds resulted in significant increase in the expression level of TLR4, IL-6, IL-8, and IL-1 β mRNA compared to that of the control group (* $P < 0.05$) as shown in Figure 14.

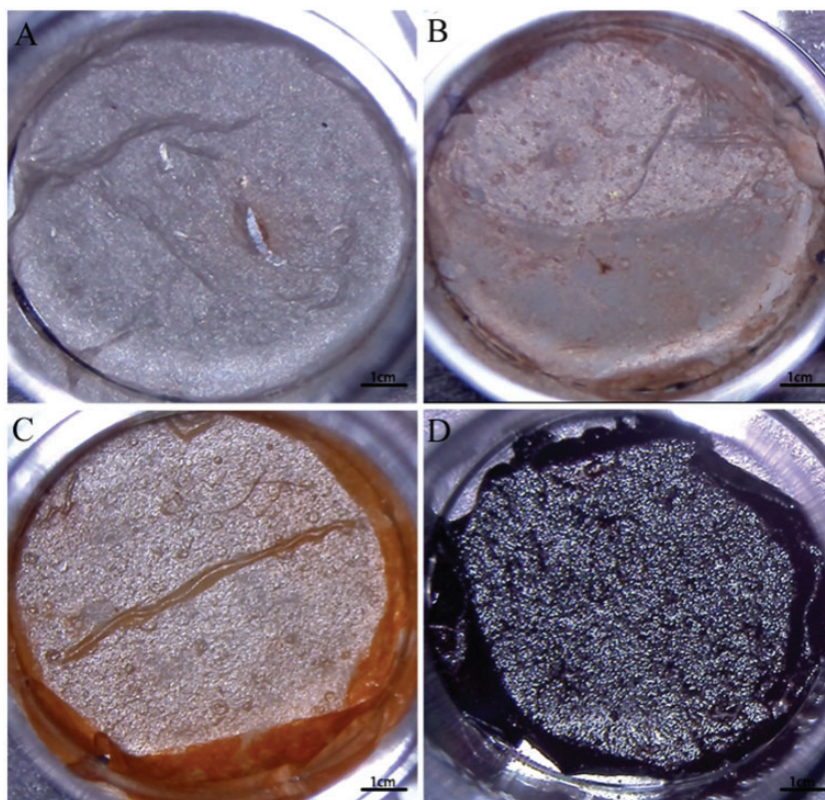


Figure 11. Formation of mineralization nodules of stereomicroscope ($\times 6$): (a) PLA; (b) PLA/CA1; (c) PLA/CA2 and (d) PLA/CA3.

Discussion

As previously reported by our group, PLA/chitosan nanofibers could promote the early proliferation of cells. However, when the content of chitosan was excessively high, fibers' surface structure was destroyed, incurring negative effect on the cell adhesion and proliferation.¹⁹ Since fibrous structure can guide periodontal tissue regeneration, such structure is commonly considered very important and therefore should be well kept for the preparation of scaffold materials. It is easier to fabricate SA into fibrous structure than chitosan, but it is a soluble polymer. On the other hand, CA has the solubility that better meets the requirements of regenerative scaffolds, and meanwhile, Ca^+ is an essential component for the regeneration of bone tissue. Taking advantage of easy conversion of Na^+ into Ca^+ via ion exchange, PLA/CA nanofibers were fabricated in this study, aimed at the preparation of a kind of stable fiber surface structure that can function as the matrix to carry calcium ions and the scaffold to embed biomaterials rather than chitosan. However, CA is known as a sort of material that has poor solubility and is present in a solid state. When PLA solution was mixed with solid CA, it is unlikely for uniform fibrous structure to develop. The SA solution is mixed with PLA solution to

obtain a stable solution. The stable mixture is prepared into fibers. PLA and CA will be evenly distributed together. Therefore, PLA/CA fibers were not prepared in this experiment straightaway. PLA/SA fibers were prepared first and then a two-step process was followed to convert them into PLA/CA fibers.

Periodontal membrane and alveolar bone are both rich in fibrous tissue; meanwhile, cementum and dentin also contain a certain amount of fibrous tissue. So fibrous tissue plays an important role in periodontal tissue. PLA, PLA/SA, and PLA/CA nanofibers are similar to the collagen fibers of periodontal tissue with fibrous structures. After soaking PLA/SA fibers in water, SA degraded and the fiber surface was no longer uniform. But the surface structure of neat PLA was not significantly altered, which exhibited certain stability (Figure 1). PLA fiber and PLA/CA fiber obtained from applying the three methods demonstrate similarity in structure, with uniformity in fiber structure and absence of beaded structure. No difference was discovered in PLA/CA fiber structures obtained from applying the three methods.

The scaffold material should have sufficient strength to support the cells' growth space, which remains firm enough during tissue regeneration. In the meantime, sufficient elasticity is also required so that cells can

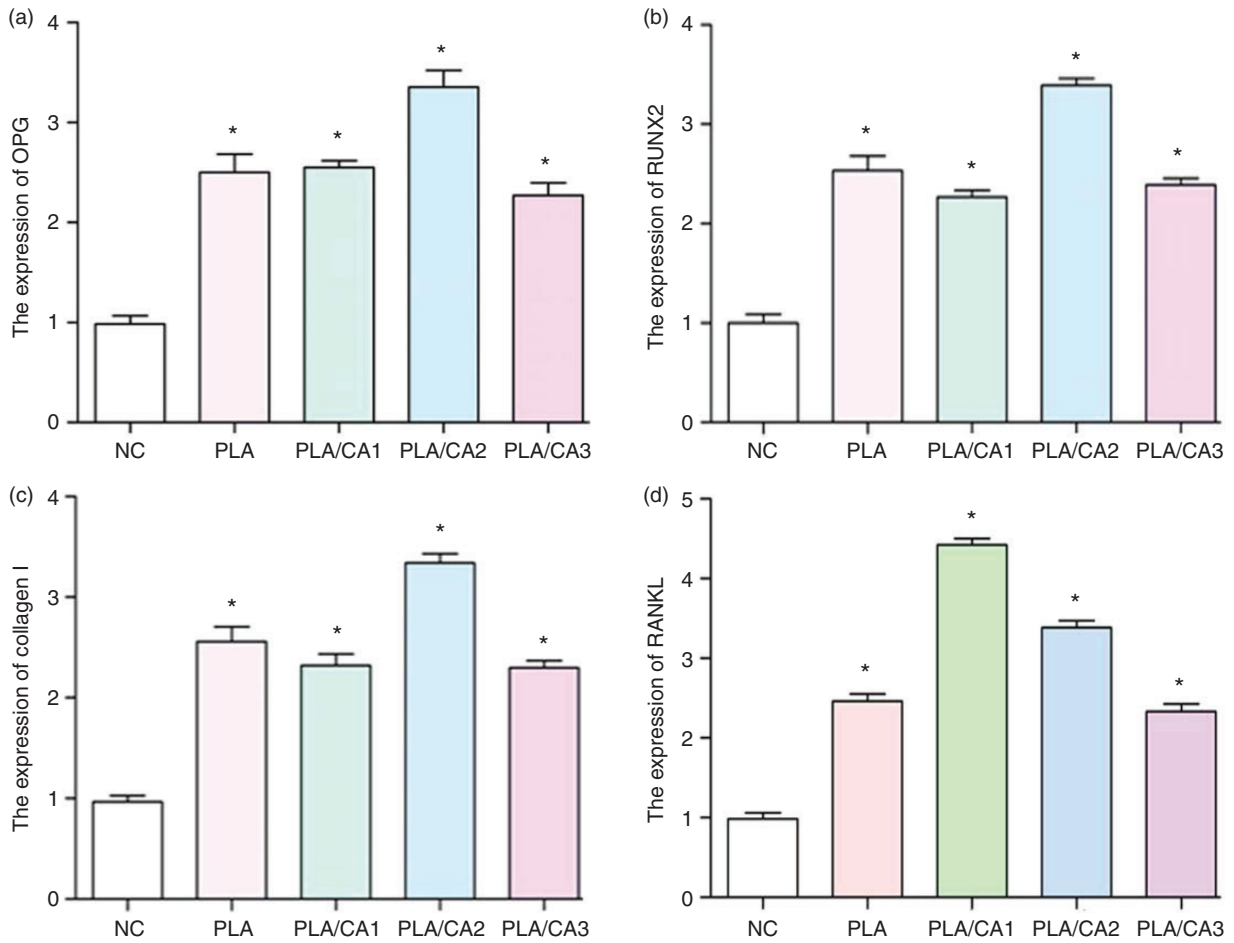


Figure 12. The expression level of BMSCs (a) OPG mRNA, (b) RUNX2 mRNA, (c) collagen I mRNA, and (d) RANKL mRNA (* $P < 0.05$, *represents a statistically significant difference with the NC group).

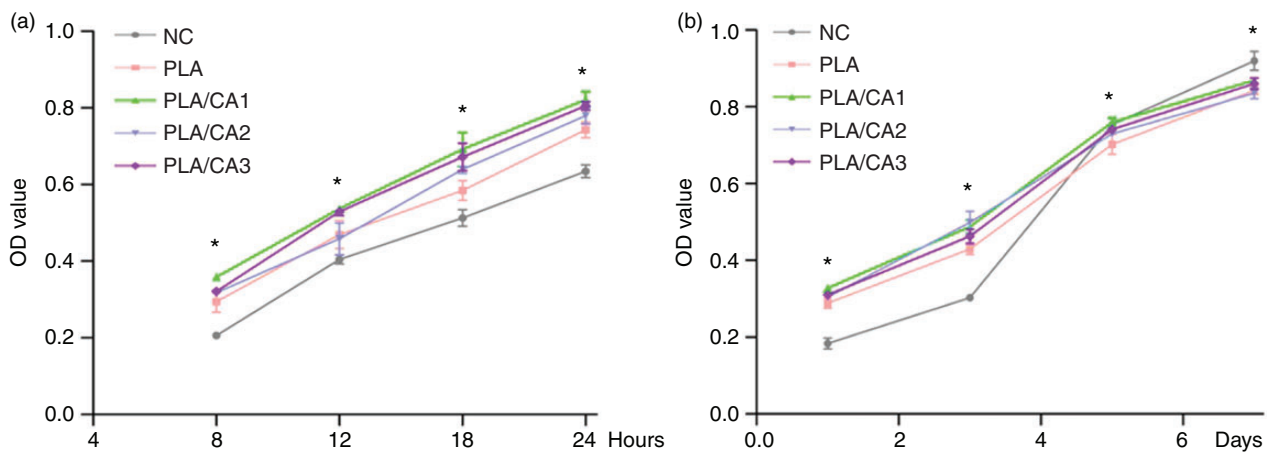


Figure 13. Proliferation of hPDLCS seeded on fibers (* $P < 0.05$, *represents a statistically significant difference with the NC group).

grow in a certain direction. Therefore, stress, elongation at break, and Young’s modulus are important indexes to evaluate the applicability of scaffolds. The mechanical strength possessed by PLA/CA fibers

prepared by our two methods is higher than that of pure PLA fibers.¹⁷ In this study, PLA/CA fibers prepared by three methods showed a high mechanical strength as compared to pure PLA fibers. Former

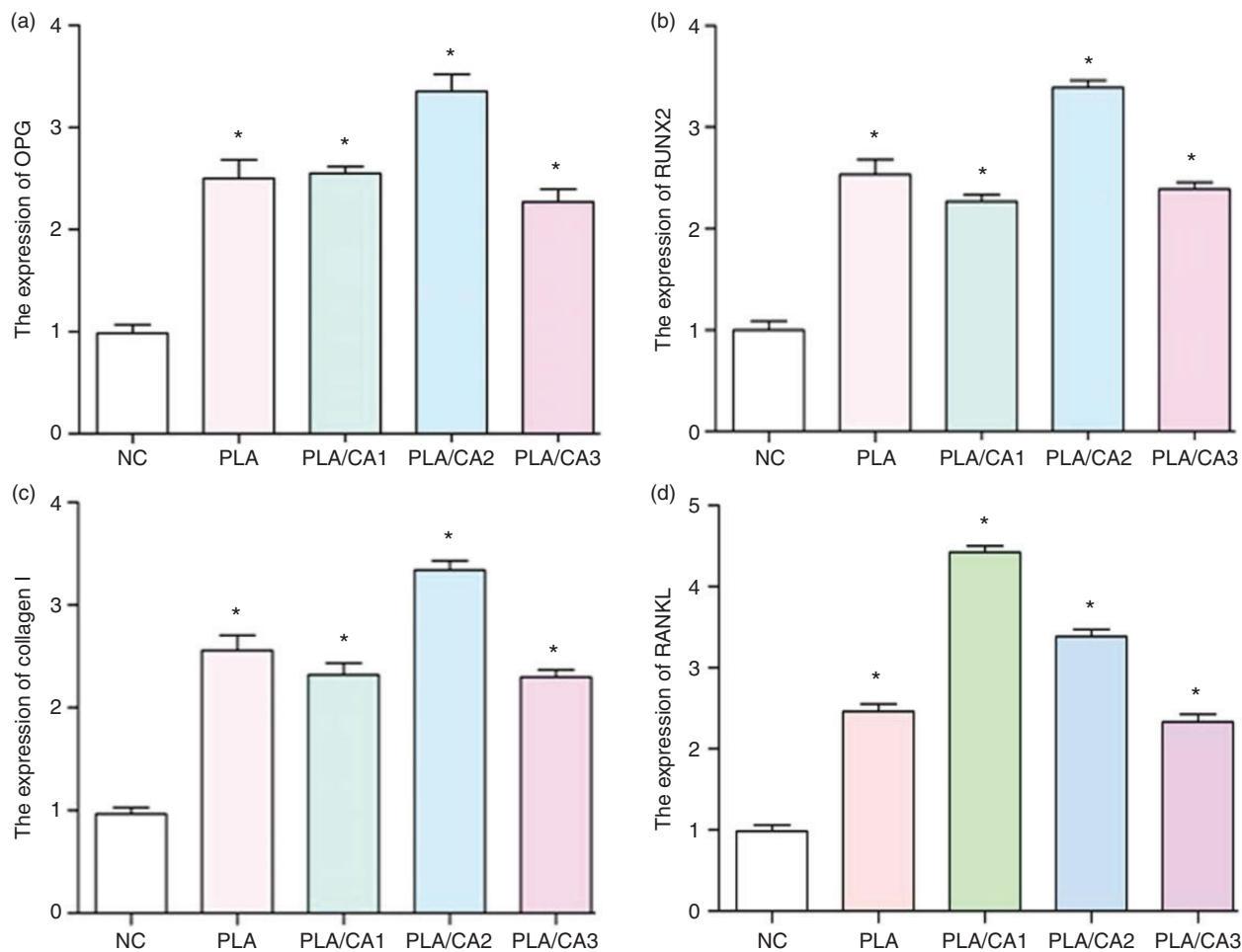


Figure 14. The expression of inflammatory genes of hPDLs: (a) IL-6; (b) IL-1 β ; (c) IL-8 and (d) TLR4 (* $P < 0.05$, *represents a statistically significant difference with the NC group).

research showed that improved strength and modulus could be obtained via adding CA into cellulose nanocrystals isolated from cotton.²⁰ The experimental results herein is consistent with the previous ones, meaning that addition of CA could enhance the scaffolds' mechanical strength and thus provide enough space for tissue regeneration. PLA/CA3 displays more desirable mechanical properties as compared to the former two materials. It is possibly due to that this method is capable to provide more calcium ions, thus enabling sodium ions to have full exchange with calcium ions. Moreover, chemical reactions are made more robust.

Results of water absorption demonstrate the increase in both WAC and WHC of fibers with the addition of CA (Figure 3), which suggests that the material could absorb more water and consequently form a more suitable environment for tissue regeneration. More tissue fluid would be stored, which could supply essential nutrients and growth factors for tissue regeneration. PLA is a hydrophobic material not easy

to store, while hydrophilic CA can contact with water more extensively and hold more water within the scaffold. In addition, CA exists with a colloidal form in water, which can further increase the water absorption and water storage performance of the material. These facts are supposed to be the reason why CA can improve the performance of PLA/CA material. There was no stark difference between PLA/CA WAC and WHC as prepared by the three methods.

As demonstrated by our prior research, PLA/CA has superior hydrophilicity to pure PLA fiber. Therefore, it was found in our study that PLA/CA fibers prepared by the three methods are extremely hydrophilic. Scaffolds' hydrophilicity was found to significantly increase when water was dropped onto the fiber surface-droplets wetted the surface of PLA/CA fiber immediately while kept the original shape on PLA fiber (Figure 4). The hydrophilicity of PLA/CA prepared by the three methods varied only insignificantly. In our previous study,¹⁹ hydrophilic chitosan was combined with PLA to greatly improve the

hydrophilicity of materials. In this experiment, CA was applied and the hydrophilicity improvement was found to be more obvious. Therefore, CA could be a material more likely to change PLA's hydrophilic energy than chitosan. As hydrophilicity is an indicator of histocompatibility, the enhanced hydrophilicity in this study demonstrated corresponding enhancement in tissue regeneration ability, cell increment, as well as cell adhesion of the obtained scaffolds.^{21–23} This result suggests that PLA/CA fibers may be more conducive to tissue growth than PLA fibers.

The degradation rate of PLA/CA fibers was found to be increased by CA without shaking. There was no significant difference in PLA/CA prepared by the three methods. One reason may be that CA could increase fibers' hydrophilicity and thus enlarge the contact area between scaffolds and water; the degradation rate was increased resultantly. Hydrophobic PLA and hydrophilic CA were immiscible, which exhibited evident phase separation in an aqueous system. Another reason can be that some CA formed hydrocolloid, which also made the scaffolds degrade faster. However, in the test of degradation rate with shaking, an opposite result was observed—the degradation rate of PLA/CA fibers was lower than that of neat PLA. This could be due to the fact that PLA possessed weaker mechanical strength and might easily be torn into pieces under shaking. The contact area between scaffolds and water was hence enlarged, raising scaffolds' degradation rate. During the process of cell growth, scaffold materials should degrade continuously to provide tissue growth space and reduce foreign body reaction. Therefore, the degradation rate is also an index for evaluating materials' performance.²⁴ There are many influencing factors, such as hydrophilicity, surface area, and porosity. In order to determine CA's effect on scaffolds' degradation rate, *in vivo* experiments were needed to conduct on animals to deduce the real situation in human body in future.

The degradation products of PLA, *i.e.* acid, may limit its wide application. Nevertheless, PLA is still proved a good biocompatible material according to extensive researches.^{25,26} As revealed in this study, the pH value of PBS solution was not significantly decreased by PLA, neither in short-term nor in long-term degradation. In the meantime, no significant increase in the pH value of PBS solution was found with the addition of alkaline molecule CA either. In short, PLA and CA may not affect tissue growth via changing pH.

BMSCs are good seed cells for transplantation and have attracted increasing attention due to their unique properties.^{27,28} Good therapeutic effects have been demonstrated in stem cell transplantation and tissue damage repair, such as osteoarthritis,²⁹ skin tissue,³⁰

cardiac diseases,³¹ etc. The regeneration of periodontal tissue is dependent on BMSCs differentiation into osteoblasts, but osteoblasts have limited ability to proliferate as a terminal cell. As a kind of stem cell, BMSCs' proliferation ability is an important factor affecting bone regeneration in periodontal tissue, so the influence from material should be systematically investigated. In our previous studies, the excessive amount of chitosan was found to destruct fiber structures, resulting in the decrease of cell proliferation and adhesion ability.¹⁹ Therefore, scaffolds' surface structure should be kept intact when increasing their hydrophilicity. As discovered by some scholars, the fibrous scaffold plays a vital role in facilitating cell proliferation,³² and using fiber scaffolds can be an effective way to mimic natural tissues, where fibrils are embedded in a matrix.³³ Herein, it was also observed that periodontal tissue and the fiber scaffold did share certain similarity of containing numerous fibers (Figure 8). Therefore, ion exchange with calcium, increasing hydrophilicity, and protecting the fibrous surface structure are the primary improvements compared to the previous PLA/chitosan system.¹⁹ In this study, neat PLA fibers were once again confirmed to enhance the BMSCs adhesion and proliferation (Figure 10), and the addition of CA could induce further promotion. The increase in cell proliferation was consistent with the results of chitosan-modified PLA,¹⁹ but such positive effect only existed in the early stages. On the seventh day, proliferation of the study group was not higher than that of the control group any more. This phenomenon has not been found in our previous studies.¹⁷ But OD value still exceeded 85%. Toxicity grading was either 0 or 1, which indicated nontoxicity of the scaffold material in line with ISO 10993–5. In addition, the proliferation curve of cells in natural state showed the typical "S" shape as that of the control group, while the cell proliferation curve was linear in the study group. Therefore, cell proliferation rate of the study group was significantly higher than that of the control group before logarithmic stage. This phenomenon has been fully demonstrated in the study of neat PLA, PLA/CA, and PLA/chitosan.¹⁹ Consequently, it can be concluded that fiber scaffolds promoted cell proliferation possibly by inducing early arrival of cells in logarithmic growth.

The regeneration of periodontal tissue originates from BMSCs differentiation into osteoblasts, which form new bone tissues to restore the periodontal tissue height. The scaffolds in this study could guide such process as one of the important approaches for periodontal tissue regeneration. Stained mineralized nodules can function as an indicator for the formation of calcified substances and also an evaluation index for the change of cell mineralization capacity. In this

research, there were barely any nodular nodules observed in neat PLA group. By contrast, PLA/CA fibers were discovered to contain a large number of red dyes with the mineralized nodules clearly distinct from those in the neat PLA group. The red staining was clearly visible in PLA/CA group, which indicated a possible rise in the number of mineralized nodules. CA is speculated to be conducive to the development of cellular mineralized nodules. Besides, this widely used biocompatible material was also proved having good effect on bone regeneration.^{34,35} Experiments further pointed out that CA could enhance the expression of mineralization genes as well as collagen (an important component of periodontal tissue).

hPDLCs are specific cells of periodontal tissue and key elements for periodontal inflammation. The pathological manifestations of periodontitis include periodontal membrane edema and inflammatory factor release, with the latter often used to evaluate the severity of inflammation.^{36,37} In this study, hPDLCs were applied as a model to inspect the inflammatory response caused by materials. Results showed that neat PLA and PLA/CA fibers all caused increase in the expression level of inflammatory mediators. No significant pH changes were observed in the one-month degradation experiment, while scaffolds could induce sharp increase to the expression level of cytoinflammatory factors within just a few days. Therefore, it might not be the pH changes that caused inflammation, but the foreign body reaction due to material itself. Then the expression of TLR4 was examined in order to find out how to reduce the material inflammation. TLR4, the surface receptor of cell membrane and an important pathway of cell inflammation, also exhibited increased expression. It has been found by our group that blocking TLR4 expression can effectively reduce cell inflammation,³⁸ and animal studies are currently in progress to check the material factor. Whether inflammation can be reduced by blocking TLR4 expression need to be confirmed in the later stage.

Authors' contribution

All authors read and approved the final manuscript.

Availability of data and materials

All data generated or analysed during this study are included in this published article.

Declaration of conflicting interests

The author(s) declared no potential conflicts of interest with respect to the research, authorship, and/or publication of this article.

Ethical approval, consent to participate and publication

The submission reported data collected from animals and human, and all studies were conducted according to the regulations for animal experimentation issued by the State Committee of Science and Technology of the People's Republic of China.

Funding

The author(s) disclosed receipt of the following financial support for the research, authorship, and/or publication of this article: This study was supported by a grant from Science and Technology Planning Project of Xiamen city (3502Z20184031), Science and Technology Planning Project of Xiamen city (3502Z20174088), Science and Technology Planning Project of Xiamen city (3502Z20174085), and Science and Technology Planning Project of Fujian province (2019j01563).

ORCID iD

Renze Shen  <https://orcid.org/0000-0001-5117-1369>

References

1. Kornman KS. Mapping the pathogenesis of periodontitis: a new look. *J Periodontol* 2008; 79: 1560–1568.
2. Bhardwaj A, Jafri Z, Sultan N, et al. Periodontal flap surgery along with vestibular deepening with diode laser to increase attached gingiva in lower anterior teeth: a prospective clinical study. *J Nat Sci Biol Med* 2018; 9: 72.
3. Sharma S, Uppoor A, Naik D, et al. Bidirectionally positioned flap technique for molar class II furcation defect – 1 year follow up. *J Ind Soc Periodontol* 2019; 23: 73.
4. Lohi HS. Comparative evaluation of the efficacy of bioactive ceramic composite granules alone and in combination with platelet rich fibrin in the treatment of mandibular class II furcation defects: a clinical and radiographic study. *J Clin Diagn Res* 2017; 11: C76–C80.
5. Sheikh Z, Hamdan N, Ikeda Y, et al. Natural graft tissues and synthetic biomaterials for periodontal and alveolar bone reconstructive applications: a review. *Biomater Res* 2017; 21: 9.
6. Lee CH, Shin HJ, Cho IH, et al. Nanofiber alignment and direction of mechanical strain affect the ECM production of human ACL fibroblast. *Biomaterials* 2005; 26: 1261–1270.
7. Yin Z, Chen X, Chen JL, et al. The regulation of tendon stem cell differentiation by the alignment of nanofibers. *Biomaterials* 2010; 31: 2163–2175.
8. Kim J, Kang MS, Eltohamy M, et al. Dynamic mechanical and nanofibrous topological combinatory cues designed for periodontal ligament engineering. *PLoS One* 2016; 11: e149967.
9. Zhou T, Liu X, Sui B, et al. Development of fish collagen/bioactive glass/chitosan composite nanofibers as a

- GTR/GBR membrane for inducing periodontal tissue regeneration. *Biomed Mater* 2017; 12: 55004.
10. Miszuk JM, Xu T, Yao Q, et al. Functionalization of PCL-3D electrospun nanofibrous scaffolds for improved BMP2-induced bone formation. *Appl Mater Today* 2018; 10: 194–202.
 11. Eğri S and Eczacıoğlu N. Sequential VEGF and BMP-2 releasing PLA-PEG-PLA scaffolds for bone tissue engineering: I. Design and in vitro tests. *Artif Cells Nanomed Biotechnol* 2016; 45: 321–329.
 12. Zhu W, Guo D, Chen Y, et al. Cytocompatibility of PLA/Nano-HA composites for interface fixation. *Artif Cells Nanomed Biotechnol* 2016; 44: 1122–1126.
 13. Stagnaro P, Schizzi I, Utzeri R, et al. Alginate-polymethacrylate hybrid hydrogels for potential osteochondral tissue regeneration. *Carbohydr Polym* 2018; 185: 56–62.
 14. Ying J, Wang P, Zhang S, et al. Transforming growth factor-beta1 promotes articular cartilage repair through canonical Smad and Hippo pathways in bone mesenchymal stem cells. *Life Sci* 2018; 192: 84–90.
 15. Żywicka B, Krucińska I, Garcarek J, et al. Biological properties of low-toxic PLGA and PLGA/PHB fibrous nanocomposite scaffolds for osseous tissue regeneration. Evaluation of potential bioactivity. *Molecules* 2017; 22: 1852.
 16. Chen L, Shen R, Komasa S, et al. Drug-loadable calcium alginate hydrogel system for use in oral bone tissue repair. *Int J Mol Sci* 2017; 18: 989.
 17. Xu W, Shen R, Yan Y, et al. Preparation and characterization of electrospun alginate/PLA nanofibers as tissue engineering material by emulsion electrospinning. *J Mech Behav Biomed Mater* 2017; 65: 428–438.
 18. Zhan X, Gao J, Liu Y, et al. Lactoferrin downregulates the expression of toll like receptor 4 stimulated by lipopolysaccharide in human periodontal ligament cells. *China J Stomatol* 2014; 32: 166–170.
 19. Shen R, Xu W, Xue Y, et al. The use of chitosan/PLA nano-fibers by emulsion electrospinning for periodontal tissue engineering. *Artif Cells Nanomed Biotechnol* 2018; 46: 419–430.
 20. Ureña-Benavides EE, Brown PJ, and Kitchens CL. Effect of jet stretch and particle load on cellulose nanocrystal-alginate nanocomposite fibers. *Langmuir* 2010; 26: 14263–14270.
 21. Kook M, Roh H and Kim B. Effect of oxygen plasma etching on pore size-controlled 3D polycaprolactone scaffolds for enhancing the early new bone formation in rabbit calvaria. *Dent Mater J* 2018; 37: 599–610.
 22. Zhu C, Lv Y, Qian C, et al. Microstructures, mechanical, and biological properties of a novel Ti-6V-4V/zinc surface nanocomposite prepared by friction stir processing. *Int J Nanomed* 2018; 13: 1881–1898.
 23. Sengupta P, Surwase SS and Prasad BL. Modification of porous polyethylene scaffolds for cell attachment and proliferation. *Int J Nanomed* 2018; 13: 87–90.
 24. Scheres N, Laine ML, de Vries TJ, et al. Gingival and periodontal ligament fibroblasts differ in their inflammatory response to viable *Porphyromonas gingivalis*. *J Periodontol Res* 2010; 45: 262–270.
 25. Nasrin R, Biswas S, Rashid TU, et al. Preparation of chitin-PLA laminated composite for implantable application. *Bioactive Mater* 2017; 2: 199–207.
 26. Diomedede F, Gugliandolo A, Cardelli P, et al. Three-dimensional printed PLA scaffold and human gingival stem cell-derived extracellular vesicles: a new tool for bone defect repair. *Stem Cell Res Ther* 2018; 9: 104.
 27. Mahla RS. Stem cells applications in regenerative medicine and disease therapeutics. *Int J Cell Biol* 2016; 2016: 1–24.
 28. Guo R, Gao L and Xu B. Current evidence of adult stem cells to enhance anterior cruciate ligament treatment: a systematic review of animal trials. *Arthroscopy* 2018; 34: 331–340.
 29. Jevotovsky DS, Alfonso AR, Einhorn TA, et al. Osteoarthritis and stem cell therapy in humans: a systematic review. *Osteoarthr Cartil* 2018; 26: 711–729.
 30. Bertozzi N, Simonacci F, Grieco MP, et al. The biological and clinical basis for the use of adipose-derived stem cells in the field of wound healing. *Ann Med Surg* 2017; 20: 41–48.
 31. Guo X, Bai Y, Zhang L, et al. Cardiomyocyte differentiation of mesenchymal stem cells from bone marrow: new regulators and its implications. *Stem Cell Res Ther* 2018; 9: 44.
 32. Ma J, He Y, Liu X, et al. A novel electrospun-aligned nanoyarn/three-dimensional porous nanofibrous hybrid scaffold for annulus fibrosus tissue engineering. *Int J Nanomed* 2018; 13: 1553–1567.
 33. Ortega Z, Aleman ME and Donate R. Nanofibers and microfibers for osteochondral tissue engineering. *Adv Exp Med Biol* 2018; 1058: 97–123.
 34. Chen C, Ke C, Yen K, et al. 3D porous calcium-alginate scaffolds cell culture system improved human osteoblast cell clusters for cell therapy. *Theranostics* 2015; 5: 643–655.
 35. Jianqi H, Hong H, Lieping S, et al. Comparison of calcium alginate film with collagen membrane for guided bone regeneration in mandibular defects in rabbits. *J Oral Maxillofac Surg* 2002; 60: 1449–1454.
 36. Ha NH, Park DG, Woo BH, et al. *Porphyromonas gingivalis* increases the invasiveness of oral cancer cells by upregulating IL-8 and MMPs. *Cytokine* 2016; 86: 64–72.
 37. Xiong H, Wei L and Peng B. The Presence and involvement of interleukin-17 in apical periodontitis. *Int Endod J* 2019; 52: 1128–1137.
 38. Mohan R, Varghese J, Bhat V, et al. The effect of non-surgical periodontal therapy on pentraxin 3 levels in smokers and nonsmokers with chronic periodontitis. *General Dentistry* 2019; 67: e1–e6.